Direct comparison of simplified models of surface reacting flows in flow chambers

P.-Y. Lagrée[1,a] and A. Ivan-Fernolendt[2]

[1] Lab. de Modélisation en Mécanique, UMR CNRS 7607, Boîte 162, Université Paris 6, 4 place Jussieu, 75252 Paris, France
[2] Department of Mathematics, University of the West Timisoara, Bv. V. Parvan, nr. 4, 1900, Timisoara, Romania

Abstract. In this paper a steady laminar 2D Poiseuille flow between two plates with chemical reactions on the upper wall is considered. This is a typical configuration in flow chambers (like the BIACORE one), which are used for the determination of the rate constants of reversible reactions between biological macromolecules. As the chamber thickness is small compared to its length, simplifications are possible, so, some asymptotic limits of mass conservation equation coupled with the wall chemistry are presented. We obtain a system with a large Péclet number. The small effects of the flow on the chemical reaction, which depend on the combination of the Damköhler and Péclet numbers, are highlighted. The results of these equations are favorably cross compared with the asymptotic (Lévêque) solution or with the simplified solutions (integral methods) found in the literature. The final result is that, due to the fact that the exchange coefficient is shown to be nearly constant, the simplified integral method is derived in a more rigorous way and its area of use is improved.

1 Nomenclature

x	longitudinal variable
$\bar{x} = x/L$	adimensional longitudinal variable
L	length of the reactor
y	transverse variable
$\bar{y} = (-y + h)/h$	adimensional transverse variable
h	thickness of the reactor
V	four times the velocity at $y = h/2$
u	velocity, Poiseuille in practice
c	concentration of the volumic reacting substance
C_T	reference value for c
d	concentration of the surfacic reacting substance
R_T	reference value for d
B	the surfacic product of the reaction
D	coefficient of diffusion
k_{on}, k_{off}	kinetic constants
$Pe = Vh^2/(DL)$,	
$Pe_h = Vh/D$	two different Péclet numbers
K	ratio $k_{off}/(k_{on}C_T)$
$Da = k_{on}R_Th/D$	Damköhler number
γ	the exchange coefficient

η	self similar variable involved in Lévêque solution
$\Gamma(x, y) = \int_y^\infty \frac{t^{-1+x}}{e^t} dt$	the incomplete Gamma function
$\Gamma(x) = \int_0^\infty \frac{t^{-1+x}}{e^t} dt$	the Gamma function

[a] e-mail: pyl@ccr.jussieu.fr

2 Introduction

The flow chambers are commonly used to measure binding rates of macromolecular interactions with a large field of biological applications (Canziani et al. (1999) [3], Karlsson et al. (1994) [12], O'Shannessy et al. (1994) [22], Schuck (1997) [27]). These chambers (such as the BIACORE device [2]) have been designed to allow the use of simple kinetic theories (for example, the experimental conditions are chosen in order to have nearly a constant spatial concentration on the "chip"). The simple theory (referred as the "integral theory") is presented at the end of this paper. Nevertheless, there are recent studies which show the limits of these theories: they present more complex theories considering the coupling between the reaction kinetics and the mass transport. They allow the understanding of the influence of the mass flux increase upon the reactions taking place on the walls. Some of them use a full system of equations (Myszka et al. (1998) [21]), some others use the asymptotic theory (Edwards (1999) [6], Edwards et al. (1999) [7]).

More complex description of a more refined inner (in the wall, and not at the surface as it will be done next) description is found in Hill and Spendiff (2000) [11], the flow being simplified in a "Triple Deck" way (Smith (1976) [29] or Saintlos and Mauss (1996) [25] or Lagrée (1999) [14]). A more complex chemistry in the flow (not only on the surface) is presented by David et al. (1999) [4] and David et al. (2000) [5].

The system rederived in the next section (Sect. 3) is classical (see Back (1975) [1], Edwards (1999) [6], Edwards et al. (1999) [7], Myszka et al. (1998) [21]), and the symbols are almost the usual ones. The choice of scales is discussed, and the non-dimensionalisation will emphasize the quasi-static behaviour of the convection/diffusion equation due to the slow reacting time. Next, a "Graetz" (Leontiev (1985) [17], Gersten and Herwig (1992) [10]) problem will be obtained after noticing that the massic Péclet number (defined here as $Pe = (4U_{max}h^2/(Dl))$ is large (Sect. 4). Next, comparisons of the two approaches are given on an example with typical numerical values, the effect of the mesh is also examined. The asymptotic limit leading to the "Lévêque" problem (Schlichting (1987) [26], Gersten and Herwig (1992) [10]) is compared with Edwards (1999) [6]. Finally (Sect. 5.3), a much more simplified set of equations (referred as the "two component" model by Myszka et al. (1998) [21]) is presented and discussed, an improved extension of this model is introduced which gives the same results as Edwards but with a larger extent of validity. In opposition with Edward approaches, in our computation, we do not have to impose a smaller than one combination of the Damköhler and Péclet numbers $DaPe^{-1/3}$. Even if the equations are classical, the cross comparison and numerical resolution are rather new, the links between the various set of equations are emphasized here and a better and more precise set of integral equation is proposed.

3 The complete equations

The fact that the basic flow is a Poiseuille one is now well established (De Bruin (2000) [8], Lorthois (1999) [18]), the entry effect is small because the Reynolds number $Re = U_{max}h/\nu$ is smaller than 20, 2D simplification holds because of the large aspect ratio (typical values can be found in the BIACORE manual [2]). Therefore, the velocity is constant along the channel and changes only in the transverse variable y:

$$u(x,y) = 4U_{max}\frac{y}{h}\left(1 - \frac{y}{h}\right), \qquad v = 0. \qquad (1)$$

Where the notation $V = 4U_{max}$ (Edwards (1999) [6]) allows to get rid of the extra number "4".
In experimental situations involving flux chambers, there is a free substance in the fluid flow ("c", of concentration $c(x,y,t)$ in the flow, named the analyte). It reacts with a ligand ("d", the receptor, of surfacial concentration $d(x,t)$) bounded to the surface of the upper wall (called the "chip"). This reaction leads to the formation of another ligand ("B" of surfacial concentration $B(x,t)$) which
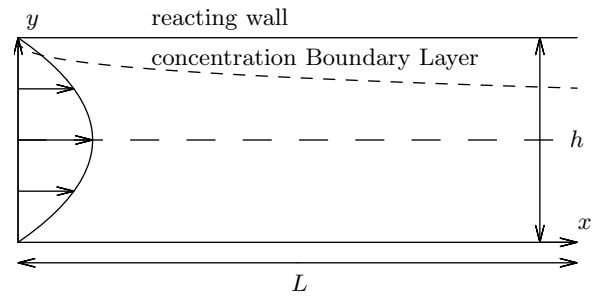

Fig. 1. A rough sketch of the Poiseuille flow. Notice that in a BIACORE cell, the chemical reaction takes place on the upper wall: $0 < x < L$, $y = h$, this is called the "chip". A concentration boundary layer develops near the upper wall, before $x = 0$ there is no reaction. The non-dimensionalisation will reverse the geometry and put the reacting wall in $\bar{y} = 0$.

is also bounded on the surface:

$$c + d \underset{k_{off}}{\overset{k_{on}}{\rightleftharpoons}} B, \qquad (2)$$

where k_{on} and k_{off} are the rate constants for the association and dissociation reactions (which are supposed independent of the flow).

A view of the configuration of the problem is presented in Figure 1.

The final problem is a set of P.D.E. and O.D.E. coupled through the boundary conditions. The substance "c" is transported through a 2D convection-diffusion process (the concentration in suspension is small so that D is constant and the velocity of the fluid is the velocity of the particles "c"):

$$\frac{\partial c}{\partial t} + u\frac{\partial c}{\partial x} = D\left[\frac{\partial^2 c}{\partial x^2} + \frac{\partial^2 c}{\partial y^2}\right] \qquad (3)$$

(u is defined by (1), the wall is always in $y = h$, the flow and the chemistry are discoupled, D is the diffusion coefficient).

The boundary conditions are:

(i) at the input, the concentration has a constant given value during the association phase:

$$c(x_{in}, y, t) = C_T, \qquad (4)$$

this value is taken to be 0 for $t > T$, the chosen time for stopping the analyte injection. Note that, as the ellipticity of equation (3) will influence the concentration field upstream of the point $x = 0$ (where the ligand "d" is disposed), a negative entrance value has to be chosen $x_{in} < 0$. In practice this effect has longitudinal and transversal scales of order $hPe_h^{-1/2}$, (with $Pe_h = Vh/D$) so it is very small, (see Sect. 5.1 and Pedley (1980) [23] for a complete discussion of the Graetz problem).

(ii) at the output it is usual to assume that the regime is "established" and that it is invariant by translation in x: $\partial_x c = 0$. This is false, except if the concentration boundary layer fills the interior of the chamber, this arises at

scale hPe_h (Pedley (1980) [23]) far larger than the effective length of the chamber L; once again, errors committed in the boundary condition will have a small effect upstream (Pedley (1980) [23]). Nevertheless this is the most simple commonly used boundary condition:

$$\frac{\partial c}{\partial x}(L, y, t) = 0, \qquad (5)$$

(iii) on the lower plate, the flux is zero, which means there is no reaction on this wall:

$$\frac{\partial c}{\partial y}(x, 0, t) = 0, \qquad (6)$$

(iv) on the upper wall, the flux of c is equal the quantity of B formed:

$$D\frac{\partial c}{\partial y}(x, h, t) = -\frac{\partial B}{\partial t}(x, t). \qquad (7)$$

A first order reaction is supposed for the creation of B:

$$\frac{\partial B}{\partial t}(x, t) = k_{on}c(x, h, t)d(x, t) - k_{off}B(x, t). \qquad (8)$$

(v) Initially, there is no substance "B", thus:

$$B(x, t = 0) = 0. \qquad (9)$$

Conservation of "d" at the wall gives:

$$d = R_T - B \qquad (10)$$

where R_T is the initial concentration of places occupied by "d" molecules. The molecules C are instantaneously provided at $t = 0$ at the entry (4):

$$c(x, y, t = 0) = 0. \qquad (11)$$

In fact, the setting of the initial time in the experiment has no real importance, because the flying time L/V is far longer than the reaction time. All these simplifications are explained in the next section, where we will observe that the asymptotic problem is in fact parabolic. Therefore there is no need for an output condition.

4 The simplifications

The first simplification comes from the choice of non-dimensionalisation of the time. At least two families are possible, one based upon the mechanics h/U_{max}, L/U_{max} or h^2D^{-1}, and another one upon the chemistry time. The first leads to values less than a second, whereas the other one leads to values of a few minutes.

So, we choose as time scale the reaction time of (8): $\tau = (k_{on}C_T)^{-1}$ (the concentration B is scaled by R_T and c by C_T). We define the relative reverse constant as: $K = k_{off}/(k_{on}C_T)$, it is mainly of order one. Of course

if K is large, the order of magnitude of the evolution time is in fact K^{-1}. As $(h/U_{max})/(k_{on}C_T)^{-1} \ll 1$ (and $(L/U_{max})/(k_{on}C_T)^{-1} \ll 1$ as well), the time derivative will disappear from the convection diffusion equation. So the ∂_t term is dropped in (3) and we obtain:

$$u\frac{\partial c}{\partial x} = D\left[\frac{\partial^2 c}{\partial x^2} + \frac{\partial^2 c}{\partial y^2}\right]. \qquad (12)$$

The velocity clearly scales with $V = 4U_{max}$. But, the choice of the distance scale is not so clear as there are two possible scales h and L. The transverse scale h comes from the fact that the boundary conditions change from the upper wall to the lower one, so we take h as transverse scale, as usual we define the $\bar{y}$ variable in order to have a reacting wall at $\bar{y} = 0$. We will notice thereafter that the proper transverse scale is not h but a thinner one because a boundary layer of concentration appears at the wall. The most simple definition of a Péclet number, is then $Pe_h = (Vh/D)$. Taking L as the longitudinal scale is in fact not the first obvious choice. A pure asymptotic (Van Dyke (1975) [30]) point of view requires that we put $x = \bar{x}h(Pe_h)$, $y = h - \bar{y}h$, $u = \bar{u}U_{max}$, in order to fulfil the "least possible degeneracy" principle of the method of "matched asymptotic expansions". So, with those scales, (12) becomes

$$\bar{y}(1 - \bar{y})\frac{\partial \bar{c}}{\partial \bar{x}} = \left[Pe_h^{-2}\frac{\partial^2 \bar{c}}{\partial \bar{x}^2} + \frac{\partial^2 \bar{c}}{\partial \bar{y}^2}\right], \qquad (13)$$

this choice of scales allows to obtain the equation with order one coefficients (least degeneracy, Van Dyke (1975) [30]), as $Pe_h \to \infty$ which is:

$$\bar{y}(1 - \bar{y})\frac{\partial \bar{c}}{\partial \bar{x}} = \frac{\partial^2 \bar{c}}{\partial \bar{y}^2}. \qquad (14)$$

This equation (with $\bar{c}$ the concentration replaced by $\bar{T}$ the temperature) is called the "Graetz problem" (with boundary condition $\bar{T}(\bar{x} = 0, 0 < \bar{y} < 1) = 0$ and $\bar{T}(\bar{x} > 0, \bar{y} = 0) = \bar{T}(\bar{x} > 0, \bar{y} = 1) = 1$, see Pedley (1980) [23], Leontiev (1985) [17] or Gersten and Herwig (1992) [10]). It solves the problem of heat transfer in a Poiseuille flow with discontinuous wall temperature (from 0 to 1 at station $\bar{x} = 0$). Equation (14) must then be solved in this natural scale ($\bar{x}$) up to any value. But, because the "final" value associated to the length L of the cell is $\bar{x} = L/(hPe_h)$ we must say that the length L scales with (hPe_h), otherwise $\bar{x}$ is 0 (because Pe_h is infinite!). Of course, in practice Pe_h has a fixed value, therefore $L/(hPe_h)$ is finite and small, but this allows to solve numerically the problem (14) for $0 < \bar{x} < L/(hPe_h)$. Nevertheless, it is more common in the flow chamber literature to use L as the longitudinal scale (so we write $x = \bar{x}L$, $y = h - \bar{y}h$), with the Péclet number defined as $Pe = \frac{Vh^2}{DL}$, (then $Pe = Pe_h\frac{h}{L}$) thus equation (12) is:

$$\bar{y}(1 - \bar{y})\frac{\partial \bar{c}}{\partial \bar{x}} = \frac{1}{Pe}\left(\frac{\partial^2 \bar{c}}{\partial \bar{y}^2} + \left(\frac{h}{L}\right)^2\frac{\partial^2 \bar{c}}{\partial \bar{x}^2}\right). \qquad (15)$$

This choice of scales allows to obtain the final equation, as $(\frac{h}{L}) \to 0$ which is:

$$\bar{y}(1-\bar{y})\frac{\partial \bar{c}}{\partial \bar{x}} = \frac{1}{Pe}\frac{\partial^2 \bar{c}}{\partial \bar{y}^2}, \qquad (16)$$

this equation must then be solved till the "final" value $\bar{x} = 1$. This way to present the equations is not relevant in "pure" asymptotic expansions because as $Pe \to \infty$, the equations degenerate again in $\bar{y}(1-\bar{y})\frac{\partial \bar{c}}{\partial \bar{x}} = 0$, which violates the least degeneracy (unless, of course, a thin Lévêque layer of relative transversal scale $Pe^{-1/3}$ is reintroduced, see Eq. (25)). Nevertheless, as we treat here an approximate problem and not an asymptotic one, we allow Pe or Pe_h to be large but finite, and the two points of view are equivalent.

Finally, we introduce the Damköhler number Da when adimensionalizing (7–8), it is $Da = k_{on}R_T h/D$ and it is of order 1. Analysing the processes near the wall, the Lévêque solution shows that there is thin layer of scale $hPe^{-1/3}$ in which the concentration changes abruptly, so the pertinent Damköhler number is in fact $k_{on}R_T hPe^{-1/3}/D$ as noted by Edwards (1999) [6]. The effect of this particular combination $DaPe^{-1/3}$ will be examined in the Edwards theory (Sect. 5.2) because it plays an important role in the validity of the simple integral models (Sect. 5.3).

4.1 Final system

With $x = \bar{x}L$, $y = h - \bar{y}h$, $u = \bar{u}4U_{max}$, (3) to (11) become at first order in Pe^{-1} (at large Péclet number):

$$\bar{y}(1-\bar{y})\frac{\partial \bar{c}}{\partial \bar{x}} = \frac{1}{Pe}\frac{\partial^2 \bar{c}}{\partial \bar{y}^2}, \qquad (17)$$

$$\bar{c}(0,\bar{y},\bar{t}) = 1, \qquad \frac{\partial \bar{c}}{\partial \bar{y}}(\bar{x},1,\bar{t}) = 0, \qquad (18)$$

$$\frac{\partial \bar{c}}{\partial \bar{y}}(\bar{x},0,\bar{t}) = Da\left[\bar{c}(\bar{x},0,\bar{t})(1-\bar{B}) - K\bar{B}\right], \qquad (19)$$

$$\frac{\partial \bar{B}}{\partial \bar{t}} = \bar{c}(\bar{x},0,\bar{t})(1-\bar{B}) - K\bar{B}, \qquad (20)$$

$$\bar{B}(\bar{x},\bar{t} = 0) = 0. \qquad (21)$$

In this system there are three adimensionalized numbers:

- $Da = \frac{k_{on}R_T h}{D}$: the Damköhler number, the ratio of the reaction rate to the diffusive rate, of order 1;
- $K = \frac{k_{off}}{k_{on}C_T}$: the rate of the reverse reaction to the direct one, also of order 1;
- $Pe = \frac{Vh^2}{DL}$: the Péclet number, which represents the ratio between diffusion and convection, large enough.

One result of this problem may be the averaged value of B on the wall, this quantity being in fact measured in the experiments and computed with:

$$\bar{\bar{B}}(\bar{t}) = \frac{1}{\bar{x}_{max} - \bar{x}_{min}}\int_{\bar{x}_{min}}^{\bar{x}_{max}} \bar{B}(\bar{x},\bar{t})d\bar{x}. \qquad (22)$$

4.2 Numerical resolution of the coupled system

The numerical resolution of (17) is done by finite elements in y and finite differences in x, the scheme is implicit in x (see Peyret and Taylor (1983) [24]). We note that the problem is parabolic therefore there is no output boundary condition. The treatment of the concentration evolution (20) is implicit in time for B and explicit in time for c. The overall precision is $O(max(\Delta\bar{y}^2, \Delta\bar{x}, \Delta\bar{t}))$. Used values for space and time steps are $\Delta\bar{y} = \Delta\bar{x} = 0.01$ and $\Delta\bar{t} = 0.01$, leading to an error of less than 2%.

5 Some direct comparisons with other models

5.1 Comparison with a complete solver: FreeFEM

5.1.1 The equations

In order to validate the simplifications of the proposed model (17–21), we present here a comparison with a complete resolution of the steady diffusive/convective problem, in the "Graetz" case, with total reaction at the wall ($Da = \infty$). It means that the simplified problem is solved here, written with the same longitudinal and transversal scale h (so that we introduce tilde variables: $x = h\tilde{x}$, $y = h\tilde{y}$, $c = C_T\tilde{c}$ and we use another Péclet: $Pe_h = Vh/D = PeL/h$):

$$\tilde{y}(1-\tilde{y})\frac{\partial \tilde{c}}{\partial \tilde{x}} = \frac{1}{Pe_h}\left[\frac{\partial^2 \tilde{c}}{\partial \tilde{x}^2} + \frac{\partial^2 \tilde{c}}{\partial \tilde{y}^2}\right] \qquad (23)$$

with boundary conditions: $\tilde{c}(\tilde{x} = -1,\tilde{y}) = 1$, $\frac{\partial \tilde{c}}{\partial \tilde{y}}(-1 < \tilde{x} < \tilde{x}_{out}, \tilde{y} = 1) = 0$,
$\frac{\partial \tilde{c}}{\partial \tilde{y}}(-1 < \tilde{x} < 0, \tilde{y} = 0) = 0$,
$\tilde{c}(0 < \tilde{x} < \tilde{x}_{out}, \tilde{y} = 0) = 0$ and $\frac{\partial \tilde{c}}{\partial \tilde{y}}(\tilde{x} = \tilde{x}_{out}, \tilde{y}) = 0$.

The resolution is done using the FreeFEM package by Lucquin and Pironneau (1996) [20], which is a finite element solver. This numerical solution is compared with the numerical solution of (17) written with h scales ($x = h\tilde{x}$, $y = h\tilde{y}$, $c = C_T\tilde{c}$, $Pe_h = Vh/D$) for sake of easier comparison:

$$\tilde{y}(1-\tilde{y})\frac{\partial \tilde{c}}{\partial \tilde{x}} = \frac{1}{Pe_h}\frac{\partial^2 \tilde{c}}{\partial \tilde{y}^2} \qquad (24)$$

with boundary conditions:
$\tilde{c}(\tilde{x} = 0,\tilde{y}) = 1$, $\frac{\partial \tilde{c}}{\partial \tilde{y}}(0 < \tilde{x} < \tilde{x}_{out}, \tilde{y} = 1) = 0$, $\tilde{c}(0 < \tilde{x} < \tilde{x}_{out}, \tilde{y} = 0) = 0$. (In fact the Damköhler number is set to a large value and $K = 0$ in equation (19) in order to obtain $\tilde{c} = 0$.)

It is well known (Schlichting (1987) [26], Gersten and Herwig (1992) [10]) that when Pe_h^{-1} and $\tilde{y}$ are small, the Lévêque solution of (24) is obtained. It means that we rescale $\tilde{y}$ near the wall with $\tilde{y} = YPe_h^{1/3}$. So, (24) is now:

$$Y\frac{\partial \tilde{c}}{\partial \tilde{x}} = \frac{\partial^2 \tilde{c}}{\partial Y^2}. \qquad (25)$$

With the selfsimilar variable $\eta = Y\tilde{x}^{-1/3}$, the self similar problem is $3f'' - \eta^2 f' = 0$ with $f(0) = 1$ and $f(\infty) = 0$,
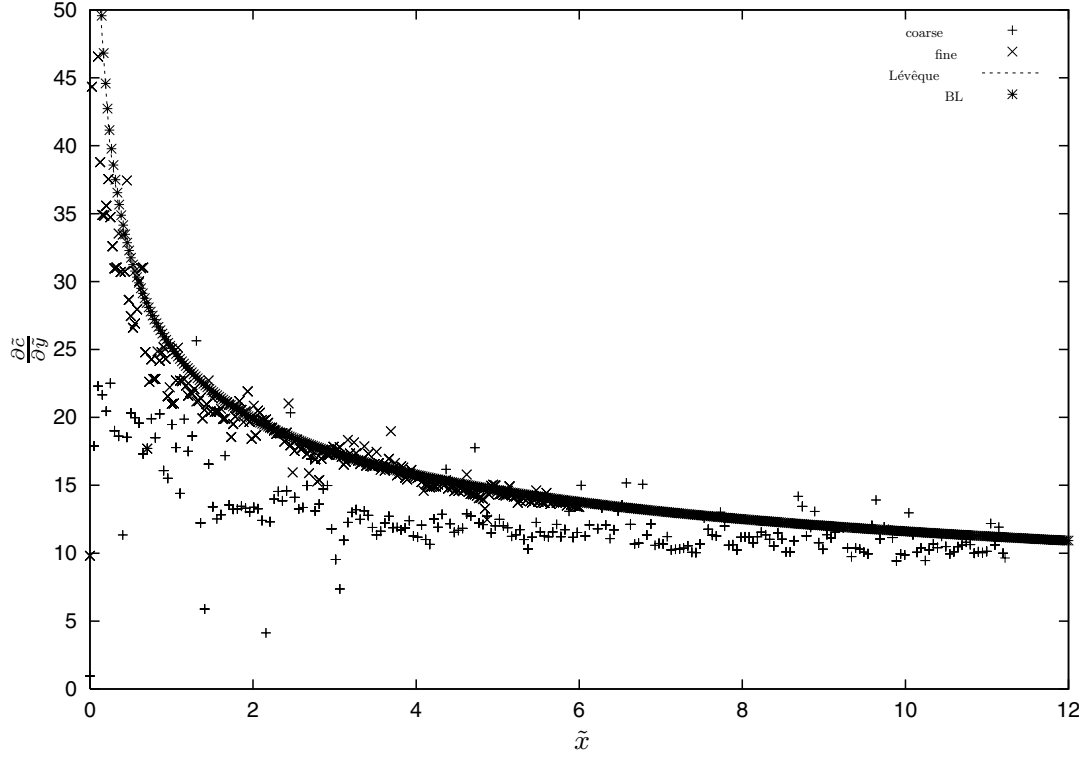
Fig. 2. Evolution of the computed value (the jagged curves are due to the numerical calculation of the derivative) of the flux $\frac{\partial \tilde{c}}{\partial \tilde{y}}$ at the wall for two grids (problem (23) with $\tilde{x}_{out} = 6$ ("fine $\times$") and 12 ("coarse $+$") and the value predicted by Lévêque $0.538(\tilde{x})^{-1/3}Pe_h^{1/3}$ (here exactly superposed with the numerical results of the problem (24) denoted "BL $*$"). Here, $\tilde{x}$ is scaled by h, $Pe_h = 100000$, $Pe = 2083$ and $Da = \infty$.

so $f(\eta) = \frac{\Gamma(\frac{1}{3},\frac{\eta^3}{9})}{\Gamma(\frac{1}{3})}$. This gives: $\tilde{c} \simeq \frac{\Gamma(1/3,(\tilde{y}Pe_h^{1/3}\tilde{x}^{-1/3})^3/9)}{\Gamma(1/3)}$. The concentration is decreasing from 1 to 0. Notice that $\Gamma(1/3,(2.92)^3/9)/\Gamma(1/3) = 0.01$, that is why is defined the "1%" value: $\delta_{1\%} = 2.92\tilde{x}^{1/3}Pe_h^{-1/3}$ (or with L and h scales: $\delta_{1\%} = 2.92\bar{x}^{1/3}Pe^{-1/3}$). This estimate is the "physical" thickness of the chemical boundary layer.

5.1.2 Results

To solve the above problem we use 240×256 grid points, we take $\tilde{x}_{out} = 12$ ("coarse") and $\tilde{x}_{out} = 6$ ("fine"). Here we focus on the entrance region: in the real BIACORE $\tilde{x}_{out}$ is about 48. The Péclet is $Pe_h = 100000$, ($Pe = 2083$). The treatment of the entrance effect needs a lot of points. It is likely that in the computations of Myszka et al. [21] (1998) there are not enough points to obtain an accurate solution near the point $x = 0$. Fortunately, the cell is very long, the numerical solution becomes valid for $x > 10h$, which is more or less the position of x_{min} the smaller abscissa of the window of optical measure, so the numerical solution will be accurate enough ($x_{min} = 0.208L$ and $x_{max} = 0.792L$). Figure 2 presents the evolution of the computed value of the flux $\frac{\partial \tilde{c}}{\partial \tilde{y}}$ at the wall for two grids (problem (23)), the value predicted by Lévêque and the numerical results of the problem (24) denoted "BL" (the last two solutions are superposed). We observe that with

the resolution of (24), we obtain exactly the Lévêque solution.

Figure 3 presents the evolution $\delta_{1\%}$ (the computed value from numerical resolution of problem (24)) compared to the predicted by Lévêque (i.e. $2.92\tilde{x}^{1/3}Pe_h^{-1/3}$). The transverse grid of Myszka et al. [21] (1998) is plotted on the same figure, showing that there may be not enough points in their computations.

As a conclusion of this sub section, we may say that our simplified diffusion equation is accurate enough and much more simple and faster to solve than the full equations.

5.2 Comparison between numerical computations, Lévêque solution and Edwards' results

In the preceding subsection we have already compared the results of system (17–21) with Lévêque solution (Schlichting (1987) [26]). In this subsection we compare the results with those with chemical reaction from David et al. (1999) [5], Edwards et al. (1999) [7] and mainly Edwards (1999) [6]. Going ahead in the asymptotics, Edwards obtained the asymptotic development of $\bar{\bar{B}}(\bar{t})$ which is:

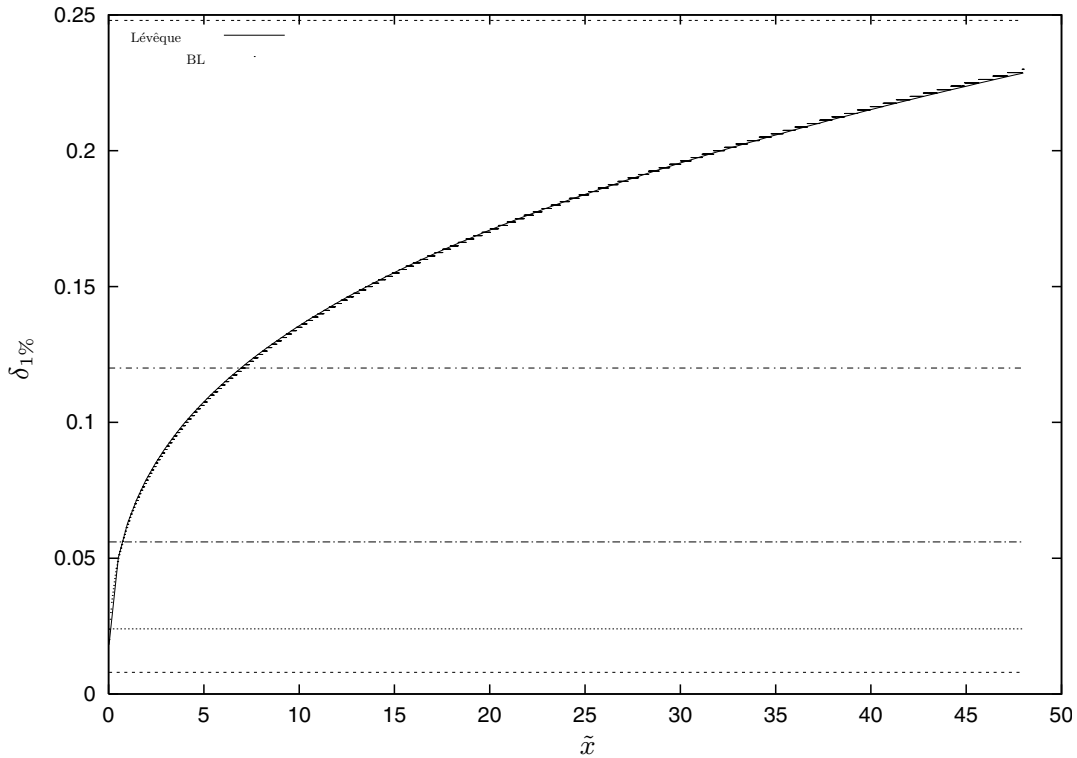$$\bar{\bar{B}} = B_0 + DaPe^{-1/3}B_1 + O((DaPe^{-1/3})^2), \quad (26)$$

Fig. 3. Evolution of the computed value of $\delta_{1\%}$ (value at which $\bar{c} = 0.01$) and the value predicted by Lévêque (here superposed with the numerical results of the problem (24) denoted "BL"). The transversal grid points from reference [21] have been plotted too, the first grid line is enough near the wall, but there are only 4 grid points in the concentration boundary layer. Here, $\delta_{1\%}$ and $\tilde{x}$ are scaled by h. $Pe_h = 100000$, $Pe = 2083$, $Da = \infty$.

with the two functions:

$$B_0 = \frac{1 - e^{-(1+K)\bar{t}}}{(1 + K)} \tag{27}$$

$$B_1 = \frac{3^{\frac{5}{3}}(x_{max}^{\frac{4}{3}} - x_{min}^{\frac{4}{3}})e^{-(1+K)\bar{t}}}{4\Gamma\left(\frac{2}{3}\right)(1 + K)(x_{min} - x_{max})}$$
$$\times \left[\frac{(e^{-(1+K)\bar{t}} - 1)}{(1 + K)} - K\bar{t}\right] \tag{28}$$

where $x_{min} = 0.208$, $x_{max} = 0.709$ (specific data for the BIACORE device ([2])); notice here that Edward's Damköhler is in fact $DaPe^{-1/3}$ (see [6]).

To test our simplified model, the averaged concentration $\bar{\bar{B}}$ defined by (22) of the reaction product is computed from (17–21). In Figure 4, $\bar{\bar{B}}$ is plotted versus adimensionalized time $\bar{t}$ for the following typical parameters: $K = 1$, $Pe = 372$ and for several Damköhler numbers ($Da = 70; 7; 3.57; 0.7; 0.072$; which correspond to $DaPe^{-1/3} = 9.7; 0.97; 0.50; 0.01; 0.001$). The Edwards (1999) [6] asymptotic development of $\bar{\bar{B}}(\bar{t})$ (26) is plotted as well.

We observe the influence of the increase of the Damköhler number upon the result. If $DaPe^{-1/3}$ is small, the prediction of Edwards and the solution of (17–21) are the same. If $DaPe^{-1/3}$ is of order one, (which arises on

the graph where $Pe = 372$ and $Da = 7$) the Edwards formula is no more valid: negative values occur. In Figure 5 is plotted the correction B_1 alone, it can be seen that even for small Pe (at small enough $DaPe^{-1/3}$) Edwards (1999) [6] gives good results. In practice $DaPe^{-1/3} = 0.5$ is a reasonable limit to obtain an accuracy of about 10%.

The conclusion of this subsection is that our model at large but finite Pe gives Edward's asymptotic solution, we even have a better description for $DaPe^{-1/3} > 0.5$.

5.3 Comparison with integral models

5.3.1 The equations

In this section, we revisit the classical integral system with the preceding results. We aim to obtain a simplified set of equations from (17–21) in taking the mean value along the reactor. Doing this, we will obtain a system with only the time as variable.

The first hypothesis is that the variations of the concentrations are negligible in x, we then define the mean longitudinal values, and suppose that the mean value of a product is nearly the product of the mean values. We draw in Figure 6 an example of the spatial distribution of $\bar{B}(\bar{x}, \bar{t})$. We notice the weak, but existing, dependence of $\bar{B}$ with $\bar{x}$, this weak dependence allows of course the proposed approximation.
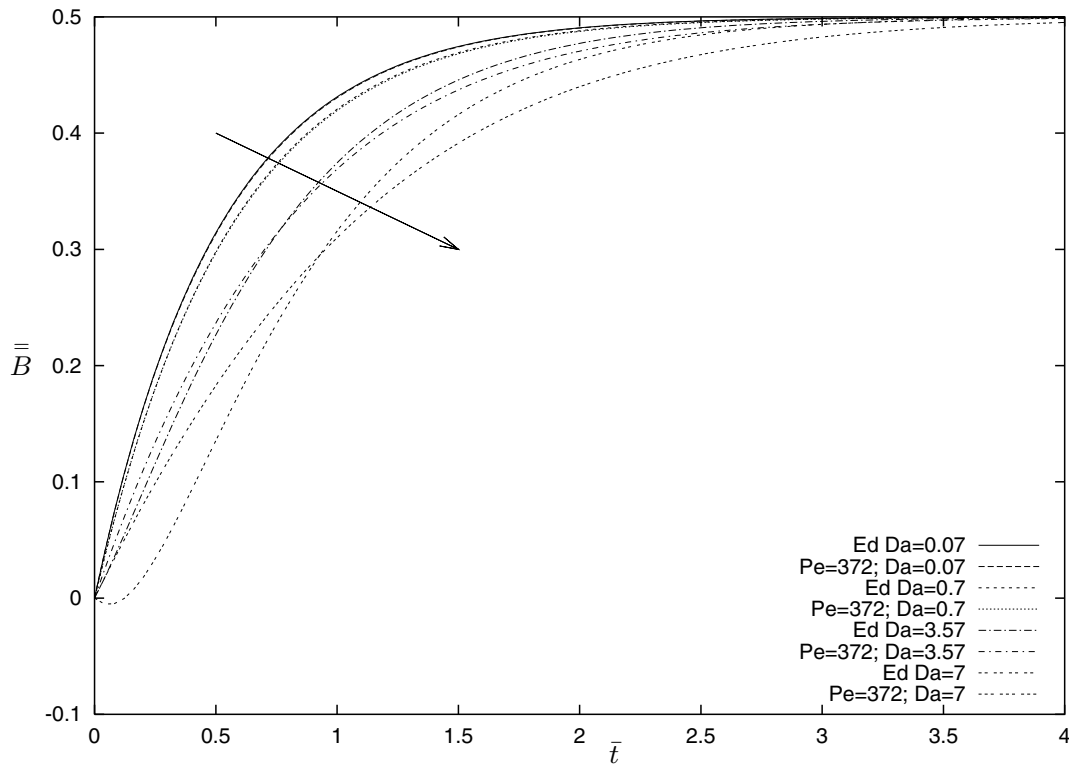
Fig. 4. The averaged concentration ($\bar{\bar{B}}$ versus $\bar{t}$) from system (17–21) at $Pe = 372$, $K = 1$ compared with $B_0 + DaPe^{-1/3}B_1$ ("Ed") for various Da ($Da = 7; 3.57; 0.7; 0.07$) leading to ($DaPe^{-1/3} = 0.97; 0.50; 0.01; 0.001$). The results are indistinguishable for $Da \ll 1$ (in practice $DaPe^{-1/3} < 0.1$). The arrow is oriented toward the growing value of Da. Edwards prediction effectively fails for $DaPe^{-1/3} \simeq 1$, the value $DaPe^{-1/3} \simeq 0.5$ induces an error of about 10%.
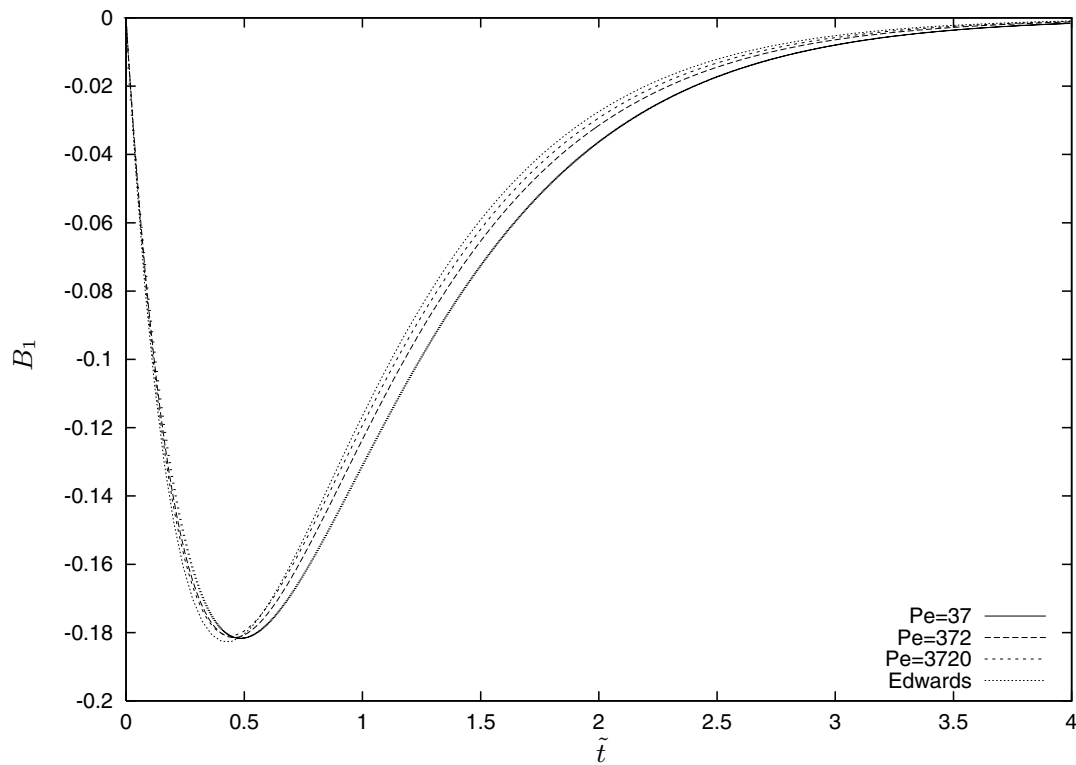

Fig. 5. The averaged correction B_1 of the asymptotic formula (26) for various Pe numbers and for $Da = 0.7$ ($DaPe^{-1/3} = 0.2$; 0.1; 0.045). Even for "small" Pe ($Pe = 37$!), but at small $DaPe^{-1/3}$, Edwards prediction is very good.
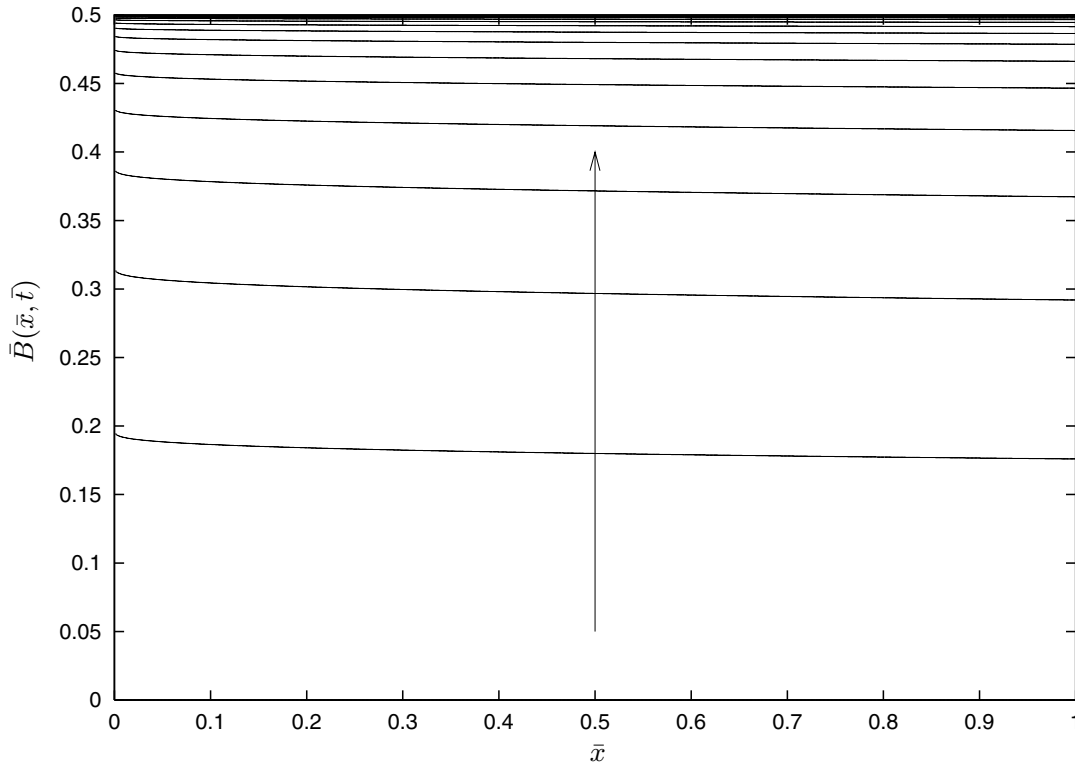
Fig. 6. One example of evolution of $\bar{B}(\bar{x}, \bar{t})$ from the resolution of (17–21), the arrow shows the direction of time, there is one curve every 0.05 time step. Parameters are: $Pe = 372$, $K = 1$ and $Da = 0.7$, so $DaPe^{-1/3} \simeq 0.1$. We notice that the distribution of $\bar{B}(\bar{x}, \bar{t})$ is not constant in $\bar{x}$, even weak.

The mean value of B (which is $L^{-1} \int dx(B)$) is denoted $\bar{\bar{B}}$, the mean value of c (which is $L^{-1} \int dx(c(x, 0, t)))$ is called C, so the average of (8) is approximated by:

$$\frac{d\bar{\bar{B}}}{dt} = k_{on} C(R_T - \bar{\bar{B}}) - k_{off} \bar{\bar{B}}. \tag{29}$$

Then the mean value of (7) gives:

$$L^{-1} \int dx \left(D \frac{\partial c}{\partial y}_{y=h} \right) = -\frac{d\bar{\bar{B}}}{dt}. \tag{30}$$

The problem is to evaluate the mean value of the flux without solving the complete problem. Two possibilities arise to estimate this flux:

• as done usually in the literature we use the Lévêque solution ($3f'' - \eta^2 f' = 0$ with $f(0) = 1$ and $f(\infty) = 0$, so $f(\eta) = \frac{\Gamma(\frac{1}{3}, \frac{\eta^3}{9})}{\Gamma(\frac{1}{3})}$), that we write here with dimensions:

$$D\frac{\partial c}{\partial y}_{y=h} = -\frac{12^{1/3}}{\Gamma(1/3)}(c - C_T) \left(\frac{x}{L}\right)^{-1/3} \frac{D}{h} \left(\frac{U_{max}h^2}{DL}\right)^{1/3}, \tag{31}$$

but this true only in the case of infinite Da and of course C_T constant. This is next averaged in x over the

length L:

$$\left\langle D\frac{\partial c}{\partial y}|_{y=h} \right\rangle = -(0.807)(C - C_T)\frac{D}{h} \left(\frac{4U_{max}h^2}{Dl}\right)^{1/3}. \tag{32}$$

• here is introduced the other limit of the Lévêque solution for small Da, this solution correspond to the case of fixed flux at the wall (rather than fixed value of c at the wall). Having imposed the flux allows to compute (we numerically solve the self similar problem $(f'' + \eta^2 f'/3 - (\eta f/3) = 0$ with $f'(0) = 1$ and $f(\infty) = 0$ so $f(\eta) = \frac{-\left(\eta \, \Gamma(-(\frac{1}{3}), \frac{\eta^3}{9})\right)}{3\,\Gamma(\frac{2}{3})}$ and $f(0) = -\left(\frac{3^{\frac{2}{3}}}{\Gamma(\frac{2}{3})}\right)$). The solution at the wall is $c = 1 - 1.54 DaPe^{-1/3}(x/L)^{1/3}$, the averaged value of $c - 1$ over x is $(0.87)^{-1} DaPe^{-1/3}$, this allows us to construct an exchange coefficient and to write the mean flux along the reactor as:

$$\left\langle D\frac{\partial c}{\partial y}|_{y=h} \right\rangle = -(0.870)(C - C_T)\frac{D}{h} \left(\frac{4U_{max}h^2}{Dl}\right)^{1/3}. \tag{33}$$

Therefore the mean value of equation (7) over the reacting wall gives for C:

$$\gamma \left(\frac{D}{h}\right)(C - C_T) \left(\frac{4U_{max}h^2}{DL}\right)^{1/3} =$$
$$\left(k_{on}C(R_T - B) - k_{off} \bar{\bar{B}}\right) \tag{34}$$

with either $\gamma = 0.807$ ($DaPe^{-1/3} \gg 1$) or $\gamma = 0.870$ ($DaPe^{-1/3} \ll 1$) The final system, ((29) and (34), but with the value 1.282 coming from the choice of the Péclet number: $0.807(4)^{1/3} = 1.282$) is called by Myszka et al. [21] (1998) the "equilibrium model" (EM). The difference is of only 10% and will be visible on our simulations but not of complete resolutions (Myszka et al. [21]).

5.3.2 The integral models

Thus, after having introduced γ the numerical coefficient of the exchange factor, we have (after solving for C as function of $\bar{\bar{B}}$ from (34) and taking (29)) with Myszka et al. (1998):

– an equilibrium model (EM):

$$C(\bar{t}) = \frac{(K\, \bar{\bar{B}}\,(\bar{t}) + \gamma(DaPe^{-1/3})^{-1})}{(1 - \bar{\bar{B}}\,(\bar{t}) + \gamma(DaPe^{-1/3})^{-1})},$$

$$\bar{\bar{B}}'\,(\bar{t}) = (1 - \bar{\bar{B}}\,(\bar{t}))C(\bar{t}) - K\, \bar{\bar{B}}\,(\bar{t}),$$

$$\bar{\bar{B}}\,(\bar{t} = 0) = 0.$$

If ($DaPe^{-1/3}$) tends to 0, we obtain from this equations

– a rapid model (RM):

$$C(\bar{t}) = 1,$$

$$\bar{\bar{B}}'\,(\bar{t}) = (1 - \bar{\bar{B}}\,(\bar{t}))1 - K\, \bar{\bar{B}}\,(\bar{t}),$$

$$\bar{\bar{B}}\,(\bar{t} = 0) = 0.$$

Nevertheless, Myszka et al. [21] (1998) exhibit another model that they called full model (FM) (or "two components system"), we write it with the reduced Damköhler ($k_M/(k_{on}R_T)$ in their notations):

– the full model (FM) (or "two components system"):

$$\bar{\bar{B}}'\,(\bar{t}) = (1 - \bar{\bar{B}}\,(t))C(t) - K\, \bar{\bar{B}}\,(\bar{t}),$$

$$C'(t) = \frac{k_{on}R_T}{(k_{on}C_T h)}(-(1 - B(\bar{t}))C(\bar{t}) + K\, \bar{\bar{B}}\,(\bar{t})$$
$$+ \gamma(Da^{-1}Pe^{1/3})(1 - C(\bar{t}))),$$

$$C(\bar{t} = 0) = 1,$$

$$\bar{\bar{B}}\,(\bar{t} = 0) = 0.$$

The problem comes from the coefficient $\frac{k_{on}R_T}{(k_{on}C_T h)}$ which does not exist in our analysis. We observe that this relative time scale is short, this allows to settle a "Bodenstein" equilibrium $C(\bar{t}) = C_e(\bar{t})$ which allows to reobtain the value of (34):

$$C_e(\bar{t}) = \frac{(K\, \bar{\bar{B}}\,(\bar{t}) + \gamma(DaPe^{-1/3})^{-1})}{\left(1 - \bar{\bar{B}}\,(t) + \gamma\left(DaPe^{-1/3}\right)^{-1}\right)}. \tag{35}$$
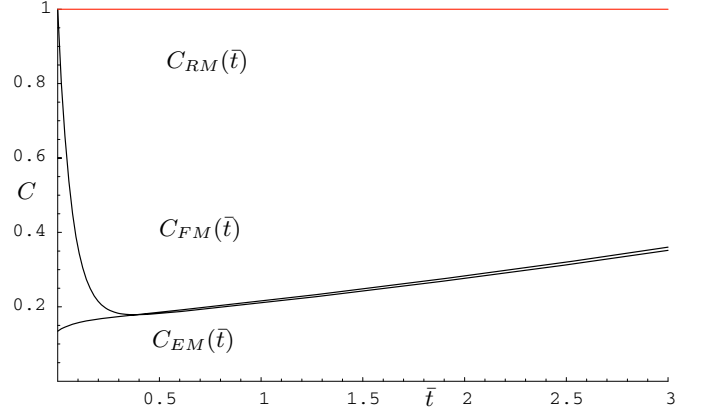

Fig. 7. Evolution of $C(\bar{t})$ for the three integral models, RM FM and EM for small time. The final value 1 is obtained for C_{EM} and C_{FM} for time $t \simeq 15$ which is not on the graph. In the FM model, there is a short time scale $\frac{(k_{on}C_T h)}{k_{on}R_T}$ at which $C_{FM}(\bar{t})$ adjusts to the curve $C_{EM}(\bar{t}) = (K\, \bar{\bar{B}}\,(\bar{t}) + 0.807(Da^{-1}Pe^{1/3}))/(1 - \bar{\bar{B}}\,(\bar{t}) + 0.807(Da^{-1}Pe^{1/3}))$. C_{RM} is 1. (Parameters $K = 0.299$, $0.807(Da^{-1}Pe^{1/3}) = 0.1556$ ($DaPe^{-1/3} = 11.7$), $\frac{k_{on}R_T}{(k_{on}C_T h)} = 12.5$, $1/(k_{on}C_T) = 3.75$ s.)

The time scale associated to the fast evolution of the concentration c is related to $h^2 D^{-1} Pe^{-2/3}$ (Edwards (1999) [6]).

In Figure 7 we observe an example of the time evolution of $C(\bar{t})$ for the three models (EM, FM and RM) at relatively small time $\bar{t}$. The relaxation to the final value of C is obtained for $t \simeq 15$ which is not on this figure. In the RM model we always have $C = 1$ (denoted C_{RM} on the plot). We note there is a quick spurious phenomena for the FM model. The concentration (denoted C_{FM} on the plot) begins at value 1 and then relaxes to the concentration C in the full model case (denoted C_{FM} on the plot). The relaxation time is of order $\frac{(k_{on}C_T h)}{k_{on}R_T}$.

5.3.3 An explicit solution

It is here to be noticed that the Rapid Model (RM) may be enhanced from the model (EM), at zero order in ($DaPe^{-1/3}$), the solution of $\bar{\bar{B}}$ in (EM) is the exponential (27). At first order in ($DaPe^{-1/3}$), C from (35) or (33) is:

$$C(\bar{t}) = 1 + \left((K + 1)\, \bar{\bar{B}}\,(\bar{t}) - 1\right)\gamma^{-1}(DaPe^{-1/3}) + \dots \tag{36}$$

so the next term in a development in powers of ($DaPe^{-1/3}$) of $\bar{\bar{B}}$ may be computed in putting (36) in (EM), and after some algebra we obtain:

$$\bar{\bar{B}} = \frac{1 - e^{-(1+K)\bar{t}}}{(1 + K)}$$
$$+ \gamma^{-1}(DaPe^{-1/3})\frac{e^{-(1+K)\bar{t}}}{(1 + K)}\left[\frac{(e^{-(1+K)\bar{t}} - 1)}{(1 + K)} - K\bar{t}\right]. \tag{37}$$
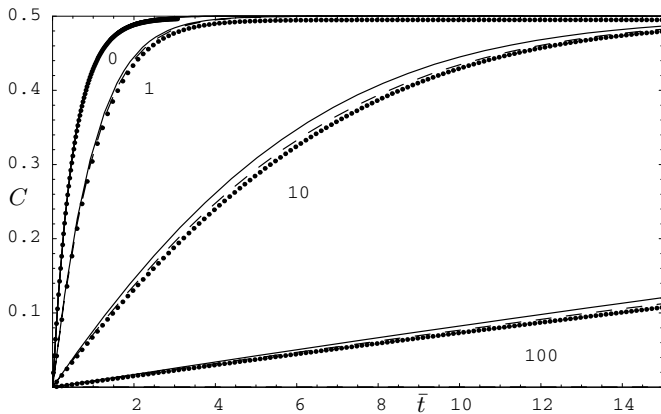
Fig. 8. Solution of (17–21): points and the equilibrium model (EM) with $\gamma = 0.87$ (line) and 0.807 (dashing) for $DaPe^{-1/3} = 0, 1, 10, 100$ and $K = 1$. For small value of $DaPe^{-1/3}$, the model (EM) with $\gamma = 0.87$ is closer to the solution of (17–21), this is not observable here but as been seen previously. As $DaPe^{-1/3}$ increases (greater than say 0.5 in practice), the model (EM) with $\gamma = 0.807$ is closer to the numerical resolution of (17–21).

This is exactly the same solution as Edwards (26) with $\gamma = 0.870$ (substituting in (28) $x_{min} = 0$; $x_{max} = 1$, one obtains $(3^{5/3}/(4\Gamma(2/3)) = 1/0.87 = 1.15)$.

5.4 Comparisons between the integral models

Finally we compare our resolution (17–21), the Rapid Model (RM) and the Equilibrium Model (EM) with $\gamma = 0.870$ and 0.807.

For small value of $DaPe^{-1/3}$, the model (EM) with $\gamma = 0.870$ is, as expected, the best description. But, as $DaPe^{-1/3}$ increases (greater than say 0.5 in practice) (EM) with $\gamma = 0.807$ is closer to the numerical resolution of (17–21). The agreement is very good for larger values of $DaPe^{-1/3}$ between (EM) with $\gamma = 0.807$ and the numerical resolution of (17–21), the error is of about 5% for $DaPe^{-1/3} = 100$. In Figure 8 we see the curves for $DaPe^{-1/3} = 0, 1, 10, 100$, for 10 and 100. The curves (EM) with $\gamma = 0.807$ and (17–21) are superposed, (EM) with $\gamma = 0.87$ gives the larger error 10%.

The conclusion of this sub section is that previous authors used an inadequate exchange coefficient. If one uses the good one, better results are obtained.

6 Conclusion and perspectives

Flow chambers were designed using simple integral theory. Asymptotic theory and full computations show now the limits of this theory and the need of a better comprehension of the influence of the flow. So, the problem we solved, consists in an imposed flow (1) in a thin channel (in a flux chamber) which transports a chemical component, this component diffuses through a Fick law giving a

mass balance equation in the flow (3). A first order reaction takes place at one of the walls (2, 8). The chemical reaction is linked to the transport equation through the boundary condition (7). A numerical code was realised in order to solve this simplified, though rich in physico-chemical phenomena, set of equations (17–21).

In the simplifications we introduced, we take into account the small aspect ratio of the reactor and the fact that the chemistry imposes its slow time. The final system (17–21) contains several non-dimensional parameters, K coming from the reverse reaction, Pe the Péclet number (ratio of convection to diffusion), and Da a Damköhler number (ratio of the chemistry flux to the diffusive flux at the wall).

In the first part, the comparisons with a resolution of the complete steady system shows that the results are accurate enough (in the case of fixed value of c at the wall). This comparison concerns only the convective-diffusive part of the equations (not the chemical part), the thickness of the reacting region is about $2.92hPe^{-1/3}$ (if $Da \gg 1$).

We have to notice that a good comparison needs a lot of mesh points and a small step size as well. Therefore model (17–21) is accurate enough because the physics lost by neglecting the elliptic part of the diffusion ($\partial_{x^2}c$) is not relevant here and is only computational time consuming, the problem being parabolic in space.

In the second part, the resolution is compared with the asymptotic analytical results of (27–28) at very large Pe (Edwards (1999) [6]), validating the chemical coupling part of the problem. From the comparisons, we see that Edwards analytical solution compares well to the solution of our system (17–21) even for moderate values of Pe if $DaPe^{-1/3}$ is smaller than one.

In the last part we revisit the simple average theory. The final "integral" comparison shows that the simplification for the flux involves a parameter γ. These expressions of the flux were based upon a large value of Da, the value of γ used previously in the literature is the good one for $DaPe^{-1/3} > 0.5$ ($\gamma = 0.807$). For smaller values ($DaPe^{-1/3} < 0.5$) a new simplification for the flux was proposed ($\gamma = 0.870$). This relation is more precise for small $DaPe^{-1/3}$ and is exactly the asymptotic result of Edwards. A systematic study may be done in order to evaluate γ as function of Pe. But the criteria (based on ($DaPe^{-1/3}$)$\lesssim 0.5$) that we propose here is precise enough for practical use.

To sum up, the flux chambers were designed with the simple integral theory, the experimental results that they provide are analyzed with these simple theories. Improvement of this theory (Myszka et al.) is not precise enough, asymptotic theory by Edwards may look too much complicated. So we have presented a simplified set of equations, and showed how the simple integral theory may be slightly changed to give better results (compared to our theory).

The next step in the modelling is the introduction of the non steady part of the convection-diffusion equation. The final step would be the construction of an inverse method (Lagrée (2000) [15]) with the final system from (Sect. 4.1), for the purpose of re obtaining all the

experimental coefficient (in a different manner than Myszka et al. (1998) [21]).

The dependence of the rate of constants k_{on} and k_{off} is believed to be dependent on the value of the skin friction at the wall, this must be included in the model. This simplified set of equations may finally be included in a model of atherosclerosis with the introduction of 3D effects (with an averaged flow in time, but with the stenosed geometry taken into account). The platelet will be the C component. At first we will look to small 3D effect in order to have a not too complicated velocity field. The rate of accumulation of the formed molecule would provide the thickening of the wall: the more B created, the more the vessel wall increases (growth of the stenosis). More reactions should be introduced to model the complex chemistry in the flow but in the vessel wall at well. This kind of approach has been already attempted by Hill and Spendiff (2000) [11].

Appendix

Here are presented typical values for the different parameters which appear in the computation

$$C_T = 10^{-11} \frac{\text{mol}}{\text{cm}^3} \qquad R_t = 4.03 \times 10^{-13} \frac{\text{mol}}{\text{cm}^2},$$

$$k_{on} = 10^8 \frac{\text{cm}^3}{\text{mol} \cdot \text{s}} \qquad k_{off} = 10^{-3} \text{ s}^{-1}$$

$$D = 28 \times 10^{-8} \frac{\text{cm}^2}{\text{s}} \qquad V = 1 \frac{\text{cm}}{\text{s}}$$

$$L = 0.24 \text{ cm} \qquad h = 5 \times 10^{-3} \text{ cm}$$

with those values $Pe = 372$, $K = 1$, $Da = 0.7$.

References

1. L.H. Back, Math. Biosci. **25**, 273 (1975)
2. BIACORE manual (undated): BIACORE^{TM} System Manual Version 1.1, Uppsala: BIACORE, Inc
3. G. Canziani, W. Zhang, D. Cines, Methods **19**, 253 (1999)
4. T. David, S. Thomas, P.G. Walker, Models of platelet deposition in stagnation point flow, presented at the *Fourth International Symposium on Computer Methods in Biomechanics and Biomedical Engineering, Oct., 1999*, pp. 13–16
5. T. David, P.G. Walker, Activation and extinction Models for Platelet adhesion, *4th Euromech Fluid Mech Conf., 19-23 Nov. 2000, Eindhoven*
6. D.A. Edwards, IMA J. Appl. Math. **63**, 89 (1999)
7. D.A. Edwards, B. Goldstein, D.S. Cohen, J. Math. Biol. **39**, 533 (1999)
8. B. de Bruin, Numerical simulation of bloodflow through straight stenotic vessels, report Rijks Universiteit Groningen/Université Paris VI, 2000
9. C.A.J. Fletcher, *Computational techniques for fluid dynamics* (Springer Verlag, 1991), Vol. II
10. K. Gersten, H. Herwig, *Strömungsmechanik* (Ed. Viewig, 1992)
11. N.A. Hill, M.K. Spendiff, Blood flow and atherosclerosis, *4th Euromech Fluid Mech Conf., 19-23 Nov. 2000, Eindhoven*
12. R. Karlsson, H. Roos, L. Fägerstam, B. Persson, Meth. Enzymol. **6**, 99 (1994)
13. P.-Y. Lagrée, Arch. Physiol. Biochem. **106** (Suppl. B), 42 (1998)
14. P.-Y. Lagrée, Int. J. Heat Mass Transfer **42**, 2509 (1999)
15. P.-Y. Lagrée, Eur. Phys. J. Appl. Phys. **9**, 153 (2000)
16. P.-Y. Lagrée, S. Lorthois, Arch. Physiol. Biochem. **107**, 51 (1999)
17. A. Leontiev, *Théorie des échanges de chaleur et de masse*, reprint of Russian ed., 1979 (Moscow, ed. MIR, 1985), 565 p.
18. S. Lorthois, Effet de la contrainte de cisaillement pariétale sur la fragmentation des caillots de fibrine. Étude expérimentale et théorique appliquée aux sténoses carotidiennes, Ph.D. thesis, 1999
19. S. Lorthois, P.-Y. Lagrée, C.R. Acad. Sci. Paris **328** (Sér. II b), 33 (2000)
20. B. Lucquin, O. Pironneau, *Introduction au calcul scientifique* (Masson, 1996), p. 380
21. D.G. Myszka, X. He, M. Dembo, T.A. Morton, B. Goldstein, Biophys. J. **75**, 583 (1998)
22. D.J. O'Shannessy, M. Brigham-Burke, K.K. Soneson, P. Hensley, I. Brooks, Meth. Enzymol. **240**, 323 (1994)
23. T.J. Pedley, *The fluid mechanics of large blood vessels* (Cambridge University press, 1980)
24. R. Peyret, T.D. Taylor, *Computational Fluid Dynamic* (Springer Verlag, 1983)
25. S. Saintlos, J. Mauss, Int. J. Eng. Sci. **34**, 201 (1996)
26. H. Schlichting, *Boundary layer theory*, 7th edn. (Mc Graw Hill, 1987)
27. P. Schuck, Annu. Rev. Biophys. Biomol. Struct. **26**, 541 (1997)
28. J.M. Siegel, C.P. Markou, D.N. Ku, S.R. Hanson, ASME J. Biomech. Eng. **116**, 446 (1994)
29. F.T. Smith, Q. J. Mech. Appl. Math. **29**, 343; 365 (1976)
30. M. Van Dyke, *Perturbation methods in fluid mechanics* (The Parabolic press, Standford, 1962)